The structure of the Ni–Fe site in the isolated HoxC subunit of the hydrogen-sensing hydrogenase from *Ralstonia eutropha*

Simone Löscher[a], Ingo Zebger[b], Lars K. Andersen[b], Peter Hildebrandt[b], Wolfram Meyer-Klaucke[c], Michael Haumann[a,*]

[a] *Freie Universität Berlin, FB Physik, Arnimallee 14, D-14195 Berlin, Germany*
[b] *Technische Universität Berlin, Institut für Chemie, Sekr. PC14, Max-Volmer-Laboratorium für Biophysikalische Chemie, Straße des 17. Juni 135, D-10623 Berlin, Germany*
[c] *DESY, EMBL Outstation, Notkestr. 85, D-22603 Hamburg, Germany*

Received 15 April 2005; revised 16 June 2005; accepted 28 June 2005

Available online 18 July 2005

Edited by Peter Brzezinski

Abstract The regulatory Ni–Fe hydrogenase (RH) from *Ralstonia eutropha* which forms a $[HoxBC]_2$ complex functions as a hydrogen sensor under aerobic conditions. We have studied a novel Strep-tag isolate of the RH large subunit, $HoxC_{ST}$, which lacks the Fe–S clusters of HoxB, allowing for structure determination of the catalytic site by X-ray absorption spectroscopy both at the Ni and, for the first time, also at the Fe K-edge. This technique, together with Fourier-transform infrared spectroscopy, revealed a Ni–Fe site with $[O_1(CysS)_2Ni^{II}(\mu\text{-}SCys)_2Fe^{II}(CN)_2(CO)]$ structure in about 50% of $HoxC_{ST}$ and a $[(CysS)_2Fe^{II}(CN)_2(CO)]$ site lacking Ni in the remainder protein. Possibly both sites may be intermediates in the maturation process of the RH.

Keywords: Bioinorganic chemistry; Ni–Fe hydrogenase; Hydrogen sensor; X-ray absorption spectroscopy

1. Introduction

The regulatory Ni–Fe hydrogenase (RH) from the β-proteobacterium *Ralstonia eutropha* is particularly interesting because it functions as a hydrogen sensor [1]. Upon cleavage of hydrogen at the Ni–Fe active site of the RH, a complex signal transduction cascade is initiated leading to the expression of the soluble and membrane-bound Ni–Fe hydrogenases which facilitate utilization of H_2 as an energy source under aerobic conditions in *R. eutropha* [2,3].

The RH reveals several unusual features which deviate from those of so-called standard Ni–Fe hydrogenases for which crystal structures are available [4,5]. The RH forms a $[HoxBC]_2$ double dimer which is connected to a tetramer of the histidine protein kinase HoxJ [6]. Each large subunit of the RH (HoxC) subunit houses a Ni–Fe active site with the Fe carrying one CO and two CN ligands [7]. The HoxB subunits presumably each bind three unusual Fe–S clusters which become reduced during H_2-cleavage [8]. H_2-cleavage activity of the RH is fully preserved in the presence of O_2 and CO [7]. The Ni–Fe site exists in only two functional states [7], namely in the as-isolated oxidized state containing Ni^{II} and in an electron paramagnetic resonance spectroscopy (EPR)-detectable Ni–C state formed in the presence of H_2, comprising a hydride-bridged Ni^{III}–H^-–Fe^{II} center [9].

In standard hydrogenases, the Ni is coordinated by two terminal CysS ligands and two μ-SCys bridges connect the Ni and Fe atoms [10]. The respective four cysteine residues are conserved in the amino acid sequences of all Ni–Fe hydrogenases [8]. Previous X-ray absorption spectroscopy (XAS) results on the RH suggested a Ni coordination by three to four CysS ligands in the oxidized state and the detachment of one CysS from Ni in the Ni–C state [11]. Whether two μ-SCys bridges are also present in the RH remained unclear.

In this study, for the first time the isolated large subunit of a Ni–Fe hydrogenase, the Strep-tag isolate of HoxC ($HoxC_{ST}$) of the RH [12], was investigated by XAS and Fourier-transform infrared spectroscopy (IR). This isolate lacks the HoxB subunits and thus the Fe–S clusters such that XAS measurements of the Ni–Fe site were possible at both the Ni K-edge and the Fe K-edge, thereby contributing to the elucidation of the atomic structure of the catalytic site.

2. Materials and methods

HoxC protein of the RH was purified from *R. eutropha* cells as a Strep-tag isolate ($HoxC_{ST}$) [12]. For XAS, protein from Strep-tag affinity chromatography was used which contains sufficiently concentrated HoxC. The preparation contains a mixture of the two forms 1 and 2 of $HoxC_{ST}$ protein that could be separated by a further gel filtration step [12]. Both forms as well as the mixture were investigated by IR spectroscopy. H_2-oxidizing activity was assayed amperometrically [3] and protein concentration according to [13]. Ni and Fe contents were quantified by atomic absorption spectroscopy (AAS) as in [8]. IR measurements were carried out on a Bruker IFS66VS spectrometer [8]. EPR was performed in the laboratory of Professor R. Bittl (FU-Berlin) on an X-band Bruker Elexsys E580 spectrometer equipped with a SHQE resonator and a helium cryostat (Oxford) (microwave frequency of 9.6 GHz). By XAS, spectra at the Ni and Fe K-edges were collected at beamline D2 of the EMBL (DESY, Hamburg, Germany). XAS

*Corresponding author. Fax: +49 30 8385 6299.
E-mail address: haumann@physik.fu-berlin.de (M. Haumann).

Abbreviations: AAS, atomic absorption spectroscopy; DCIP, 2,6-dichlorophenolindophenol; EPR, electron paramagnetic resonance spectroscopy; EXAFS, extended X-ray absorption fine structure; IR, infrared spectroscopy; HoxC, large subunit of the RH; $HoxC_{ST}$, Strep-tag isolate of HoxC; RH, regulatory Ni–Fe hydrogenase; XANES, X-ray absorption near-edge structure; XAS, X-ray absorption spectroscopy

0014-5793/$30.00
doi:10.1016/j.febslet.2005.06.063

samples contained 10 μL of protein (~0.3 mM) solution. Fluorescence-detected XAS spectra were measured with a 13-element Germanium detector (Canberra) at 20 K [11]. An absolute energy calibration (accuracy ±0.1 eV) was performed by the Bragg-reflections method [14]. Five scans of ~45 min duration were taken on the same spot of the sample; 10 scans from 2 separate spots were averaged for each extended X-ray absorption fine structure (EXAFS) spectrum. Spectra were normalized and EXAFS oscillations were extracted as in [15]. Unfiltered k^3-weighted spectra were used for least-squares curve-fitting [15] and for calculation of Fourier-transforms representing k-values between 1.85 and 13 $Å^{-1}$. Data were multiplied by a fractional cosine window (10% at low and high k-side); the amplitude reduction factor S_0^2 was 0.9. The same samples were subjected first to EPR and then to XAS measurements. Multiple-scattering X-ray absorption near-edge structure (XANES) calculations were performed as in [16] using the ab initio code FEFF 8.2 [17] with the full-multiple-scattering (FMS) and the self-consistent-field (SCF) options activated [16]. Atomic coordinates of FEFF input files for XANES calculations were generated using the Ni-ligand distances from EXAFS simulations and employing the atomic structure of the Ni–Fe site from *Desulfovibrio gigas* [4] as a template.

3. Results

AAS analysis of three independent preparations of isolated $HoxC_{ST}$ revealed a Ni/Fe ratio of 0.48 ± 0.07 and about one Fe ion per protein. The presence of the diatomic ligands of the Fe of the Ni–Fe site, one CO and two CN, was verified by IR spectroscopy [7,16]. The IR spectrum of the isolated $HoxC_{ST}$ preparation and those of its two separated forms (see [12]) are nearly identical (Fig. 1). However, the spectra

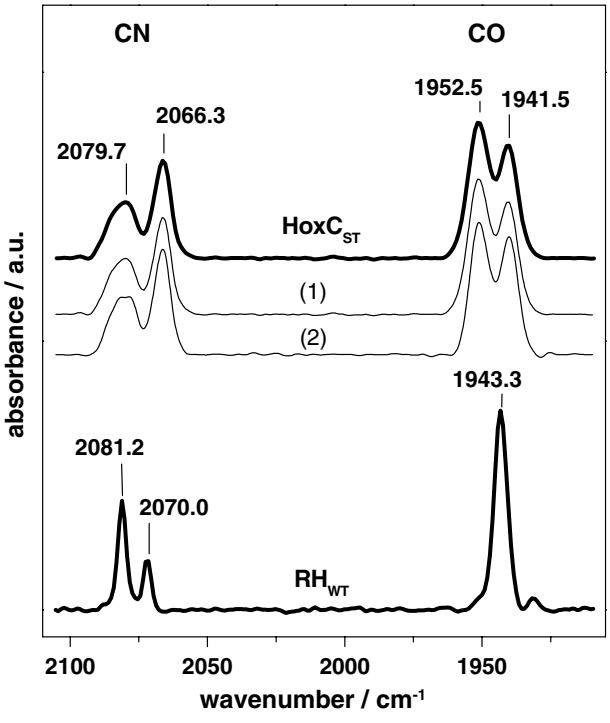

Fig. 1. IR spectra of isolated $HoxC_{ST}$ (top) and wild-type double dimeric RH_{WT} (bottom) in the oxidized state [8] in the region of the CO and CN stretching modes. The spectrum of $HoxC_{ST}$ refers to a sample including the two forms (1) $(HoxC_{ST})_2$–HypBC complex and (2) $(HoxC_{ST})_2$ as identified in [12]. The spectra of the separated forms (1 and 2) are shown for comparison.

differ significantly from that of native, double dimeric RH, which displays one relatively sharp band originating from the CO stretching mode and two bands from the CN stretching modes. In contrast, two bands in the CO stretching region are observed in $HoxC_{ST}$ and also the broad and asymmetric band envelopes in the CN stretching region point to the involvement of more than two bands. These results indicate that $HoxC_{ST}$ includes at least two different types of metal centers.

Taking into account the AAS results one may assume that only ca. 50% of $HoxC_{ST}$ contains a fully assembled Ni–Fe center whereas in the remainder, the Ni is missing, but the CN and CO ligands are already coordinated to the Fe. The agreement of the IR spectra of the separated forms and the isolated $HoxC_{ST}$ indicates that the coordination pattern of the Fe site is the same regardless of the Ni content and of HypBC binding [12]. A band fitting analysis provides a satisfactory description of the IR spectrum of $HoxC_{ST}$ using four and two bands in the CN and CO stretching regions, respectively. However, it was not possible to simulate the experimental IR spectrum on the basis of the components in the spectrum of double dimeric RH plus an additional set of bands for two CN and one CO stretching modes. Thus, we conclude that the Fe site not only of the Ni-deficient and but also of the fully assembled $HoxC_{ST}$ exhibits different structural and electronic properties as compared to the native RH. The lack of the Ni ion is likely to have a distinct impact on the geometry and electron density distribution in the $Fe(CN)_2(CO)$ complex and thus on the CN and CO stretching frequencies. Hence, the CO stretching of the Ni-deficient $HoxC_{ST}$ is assigned to the 1952.5-cm^{-1} band since it displays the largest shift compared to the native enzyme. More surprising, however, are the spectral discrepancies between the Ni-containing $HoxC_{ST}$ and the intact RH, which may result from a different ligation pattern of the Ni (vide infra), or from the effect of the different quaternary structures, since $HoxC_{ST}$ lacks the small HoxB subunit and the HoxC subunit tends to dimerize [12].

In double dimeric RH, H_2-binding at the Ni–Fe site is detectable by a shift of ν(CO) of about 18 cm^{-1} to higher frequencies and by the formation of the paramagnetic Ni–C state of the protein [7,8]. Neither the ν(CO) shift nor the Ni–C EPR signal were observed in preparations of $HoxC_{ST}$ flushed with H_2 for 10 min (data not shown), that is under conditions, which cause quantitative reduction of native RH. The IR and EPR spectra of $HoxC_{ST}$ were also not affected by the addition of dithionite as a strong reductant or by adding 2,6-dichlorophenolindophenol (DCIP) as an external oxidant. Thus, the Ni–Fe site in isolated $HoxC_{ST}$ seems to be redox-inactive.

XAS at the Fe and Ni K-edges provides information on the atomic structure of both the Fe and Ni sites [15,18]. The Fourier-transform (FT) of the Fe EXAFS spectrum of $HoxC_{ST}$ (Fig. 2A) shows two prominent peaks immediately revealing at least two shells of backscatterers likely due to Fe–C(N/O) and Fe–S(cysteine) interactions. A simulation of the spectrum assuming three C(N/O) ligands, only one SCys ligand, and the presence of Ni in half of the protein yielded an unrealistically small Debye–Waller parameter for the sulfur shell (Table 1) and a large error factor (R_F). The inclusion of two S-ligands largely improved the fit result so that R_F was diminished by a factor of three. Assuming one further O-ligand to Fe insignificantly decreased the R_F-value (by <2%). Thus, the relatively

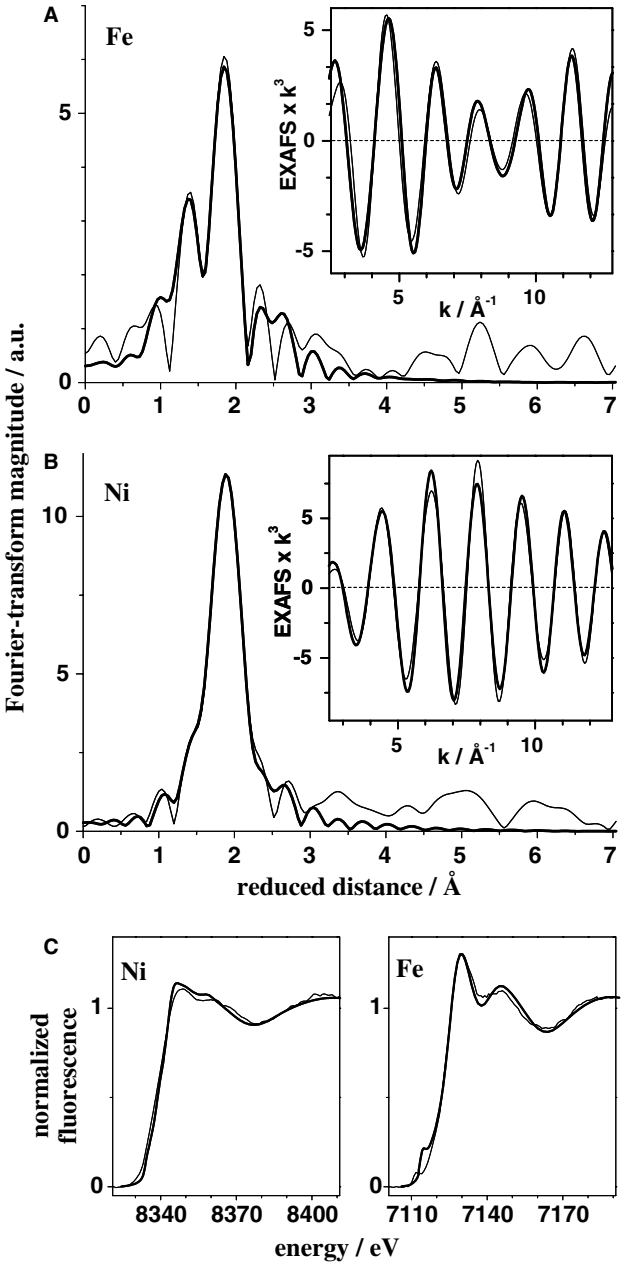

Fig. 2. XAS spectra of $HoxC_{ST}$ at the Ni and Fe K-edges. Fourier-transforms (thin lines) of (A) Fe and (B) Ni experimental EXAFS spectra. EXAFS oscillations in the insets (thin lines) represent backtransforms of Fourier-isolations over 1–3 Å of reduced distance to obtain noise-free spectra for better visual comparison with the simulations. Thick lines show simulation results (Table 1) of fit II (in A) and of fit IV (in B). (C) Thin lines: experimental Ni (left) and Fe (right) XANES spectra; thick lines: XANES simulations according to a structural model constructed on basis of a Ni–OS_4 configuration, using the Ni, Fe-ligand distances in Table 1 of fit IV (left) and fit II (right), and employing the geometry of the Ni–Fe site in the crystal structure of *D. gigas* hydrogenase [4] as a template.

large Debye–Waller factor of the C(N/O) shell may not result from a further oxygen ligand to the Fe, but from an increase of the Fe–CN distance by ca. 0.1 Å compared to the Fe–CO distance [4], and/or from slightly different Fe–C(N/O) distances in the absence or presence of Ni. Both simulations yielded a Fe–Ni distance of ~2.64 Å (Table 1). Clearly, the Fe EXAFS data suggest the presence of two SCys ligands to Fe. They are furthermore compatible with three CN/CO Fe-ligands in the whole $HoxC_{ST}$ protein in line with the IR data whereas no evidence for oxygen ligation to Fe was obtained. Consequently, Ni (when present) and Fe are connected by two μ-SCys bridges in isolated $HoxC_{ST}$; the presence of a bridging oxygen species is less likely.

The Ni EXAFS spectrum of $HoxC_{ST}$ (Fig. 2B) is largely similar to the that of HoxC of oxidized double dimeric RH [11]. However, the XANES edge maximum (Fig. 2C, left) was found to be slightly higher and the pre-edge peak is less well resolved. In previous investigations, the number of sulfur ligands to the Ni in the RH remained uncertain [11]. In this study, simulation of the Ni EXAFS was improved by using the Ni–Fe distance of 2.64 Å independently derived from the Fe EXAFS as a fixed parameter. For this approach, a single fit minimum was only obtained if two shells of S-ligands with significantly different lengths were employed. This result is reasonable since two S-shells, the longer from one of the two Ni–μ-SCys interactions, have also been obtained in XAS investigations on standard Ni–Fe hydrogenases [19].

Simulation of the Ni EXAFS of $HoxC_{ST}$ assuming tetracoordinated Ni with OS_3 or S_4 ligation yielded relatively large fit errors ($R_F > 12\%$) (Table 1). The shape of the XANES spectrum (see below) is also better compatible with five-coordinated Ni [20]. Both, O_2S_3 and OS_4 EXAFS simulations provided largely improved fits ($R_F < 6\%$) (Table 1). To discriminate between these Ni coordinations, quantitative XANES simulations were performed [16]. Simulations using the EXAFS-derived Ni-ligand distances (Table 1) and O_2S_3 coordinated Ni yielded a primary maximum of the Ni K-edge that was significantly too large (not shown), whereas a simulation on the basis of a OS_4 Ni-coordination is in better agreement with the experimental spectrum (Fig. 2C, left). The edge maximum in a XANES simulation with S_4 Ni-coordination (not shown) was slightly smaller than in the experimental spectrum, however, more similar to that of native oxidized RH [11]. A simulation of the Fe XANES on basis of the likely C_3S_2 coordination well reproduced the overall shape of the experimental spectrum (Fig. 2C, right). The excess pre-edge peak magnitude may be due to limitations of the muffin-tin potential approximation in the FEFF code at low edge energies [15] for transition metals with partially filled 3d orbitals [21,22]. Notably, both the Fe and the Ni XAS data indicate a homogeneous ligand environment of the metals, in line with the suggestion that the heterogeneity in the IR spectrum is due to the lack of Ni in about half of $HoxC_{ST}$.

4. Discussion

The isolated large subunit HoxC of the RH [12] allows in-depth elucidation of the atomic structure and assembly process of the Ni–Fe active site of the oxygen-insensitive hydrogen sensor. The data are best explained assuming that in about 50% of the $HoxC_{ST}$ samples studied in this work, Ni is incorporated whereas in the remainder protein Ni is missing. Despite this heterogeneity, the spectroscopic data demonstrate the binding of the $Fe(CN)_2(CO)$ complex, both in the presence and absence of the Ni. This observation provides direct evidence that the $Fe(CO)(CN)_2$ site is assembled prior to the incorporation of Ni in the intricate maturation process of the RH involving the accessory Hyp proteins [12,23].

Table 1
Simulation results of Fe and Ni EXAFS oscillations of isolated $HoxC_{ST}$ protein

		Shell	N_i (per metal)	R_i (Å)	$2\sigma_i^2$ (Å^2)	R_F (%)
Fe	Fit I/II	C	3*/3*	1.98/1.91	0.022/0.014	23.4/8.5
		S	1*/2*	2.26/2.25	<0.001/0.007	
		Ni	0.5*/0.5*	2.64/2.64	0.006/0.006	
Ni	Fit III/IV/V/VI	O	1*/1*/–/2*	2.03/2.03/–/2.08	0.002*/0.002*/–/0.004	12.6/5.1/14.8/5.2
		S	2*/3*/3*/2*	2.28/2.28/2.26/2.30	<0.001/0.004/0.005/0.002	
		S	1*/1*/1*/1*	2.61/2.59/2.60/2.60	0.004*/0.004*/0.004*/0.004*	
		Fe	1*/1*/1*/1*	2.64*/2.64*/2.64*/2.64*	0.008/0.007/0.006/0.007	

N_i, coordination number; R_i, absorber–backscatterer distance; $2\sigma_i^2$, Debye–Waller parameter; R_F, error value calculated as defined in [25] over reduced distances ranging from 1.3 to 2.5 Å.
*Parameters that were kept constant in the simulations.

The XAS results indicate that two cysteine side chains are coordinated to the Fe, which, after incorporation of Ni, presumably serve as bridging ligands between both metal ions in $HoxC_{ST}$. The CO stretching of the Ni-containing $HoxC_{ST}$ that is attributed to the 1943.3 cm^{-1} band exhibits only a 1.8 cm^{-1} downshift compared to that of native RH whereas a distinctly larger shift would be expected for a different number of Fe-ligating thiols. Thus, two μ-SCys bridges likely are present also in oxidized native RH, solving a previously open question [11]. Improved analysis employing both Ni and Fe XAS data favors Ni coordination by four CysS ligands in total, similar to standard Ni–Fe hydrogenases, in $HoxC_{ST}$. Whether two terminal cysteines are also present in the oxidized native RH remains less clear.

Despite the same bridging mode by cysteines, the structure of the completely assembled Ni–Fe site of $HoxC_{ST}$ is not fully identical to that of HoxC in native RH as revealed by the IR and XANES spectra. In the native RH, H_2-binding leads to the Ni–C state, where a hydride bridges the Ni and the Fe ion [9,11]. In isolated $HoxC_{ST}$, the Ni–C state is not accessible. The XAS data reveal the presence of at least one oxygen ligand at the Ni in $HoxC_{ST}$. Like in oxidized standard hydrogenases [24], an oxygen may bridge the Ni and Fe atoms, thereby blocking the binding site for H_2. However, the Fe XAS of $HoxC_{ST}$ provides no evidence for oxygen ligation to the Fe; also H_2 activity was not observed under strongly reducing conditions which should remove the bridging oxygen [16]. Thus, $HoxC_{ST}$ presumably lacks a bridging oxygen. Instead, $HoxC_{ST}$ may include a terminal oxygen at the Ni which is possibly not present in the native RH [11], and this may be the origin for the small shift of the CO stretching frequency ν(CO) in the IR spectrum (vide supra). Hence, not only the Ni-deficient protein but also the Ni-containing $HoxC_{ST}$ may represent intermediates in the maturation process [12].

In the native RH, Ni–C state formation is accompanied by the reduction of Fe–S clusters in the small subunit HoxB [8]. In $HoxC_{ST}$, such an electron transfer certainly is impossible due to the lack of the Fe–S clusters. In conclusion, the Ni-bound oxygen species, a different Ni ligation by terminal thiols, and/or the inability to transfer at least one electron from the Ni–Fe site to the Fe–S clusters seem to prevent Ni–C state formation in $HoxC_{ST}$.

In summary, we propose a $[O_1(CysS)_2Ni^{II}(\mu\text{-}SCys)_2Fe^{II}(CN)_2(CO)]$ configuration of the Ni–Fe site in completely assembled isolated $HoxC_{ST}$. With respect to the $(\mu\text{-}SCys)_2$ bridging of Ni and Fe, this configuration seems to hold also for the oxidized native RH.

Acknowledgments: We thank Dr. T. Buhrke and G. Winter from the workgroup of Prof. B. Friedrich (HU-Berlin) for providing the RH preparations and for intense collaboration and Prof. H. Dau (FU-Berlin) for generous support. The EMBL Outstation Hamburg is acknowledged for excellent support, Prof. R. Bittl and Dr. C. Kay (FU-Berlin) for help with the EPR experiments, and Dr. K. Irrgang (TU-Berlin) for kind assistance in AAS. Financial support from the Deutsche Forschungsgemeinschaft within SFB 498 (C8, A8) is gratefully acknowledged.

References

[1] Lenz, O. and Friedrich, B. (1998) A novel multicomponent regulatory system mediates H_2 sensing in *Alcaligenes eutrophus*. Proc. Natl. Acad. Sci. USA 95, 12474–12479.
[2] Lenz, O., Bernhard, M., Buhrke, T., Schwartz, E. and Friedrich, B. (2002) The hydrogen-sensing apparatus in *Ralstonia eutropha*. J. Mol. Microbiol. Biotechnol. 4, 255–262.
[3] Pierik, A.J., Schmelz, M., Lenz, O., Friedrich, B. and Albracht, S.P. (1998) Characterization of the active site of a hydrogen sensor from *Alcaligenes eutrophus*. FEBS Lett. 438, 231–235.
[4] Volbeda, A., Charon, M.H., Piras, C., Hatchikian, E.C., Frey, M. and Fontecilla-Camps, J.C. (1995) Crystal structure of the nickel–iron hydrogenase from *Desulfovibrio gigas*. Nature 373, 556–557.
[5] Frey, M. (2002) Hydrogenases: hydrogen-activating enzymes. Chem. Biochem. 3, 153–160.
[6] Buhrke, T., Lenz, O., Porthun, A. and Friedrich, B. (2004) The H_2-sensing complex of *Ralstonia eutropha*: interaction between a regulatory [NiFe] hydrogenase and a histidine protein kinase. Mol. Microbiol. 51, 1677–1689.
[7] Bernhard, M., Buhrke, T., Bleijlevens, B., De Lacey, A.L., Fernandez, V.M., Albracht, S.P. and Friedrich, B. (2001) The H_2 sensor of *Ralstonia eutropha*. J. Biol. Chem. 276, 15592–15597.
[8] Buhrke, T., Löscher, S., Schlodder, E., Zebger, I., Andersen, L.K., Hildebrandt, P., Meyer-Klaucke, W., Dau, H., Friedrich, B. and Haumann, M. (2005) Reduction of unusual iron–sulfur clusters in the H_2-sensing regulatory Ni–Fe hydrogenase from *Ralstonia eutropha*. J. Biol. Chem. 280, 19488–19495.
[9] Brecht, M., Van Gastel, M., Buhrke, T., Friedrich, B. and Lubitz, W. (2003) Direct detection of a hydrogen ligand in the [NiFe] center of the regulatory H_2-sensing hydrogenase from *Ralstonia eutropha* in its reduced State by HYSCORE and ENDOR spectroscopy. J. Am. Chem. Soc. 125, 13075–13083.
[10] Cammack, R., Robson, R. and Frey, M., Eds., (1997). Hydrogen As a fuel: Learning From Nature, Taylor & Francis, London, UK.
[11] Haumann, M., Porthun, A., Buhrke, T., Liebisch, P., Meyer-Klaucke, W., Friedrich, B. and Dau, H. (2003) Hydrogen-induced structural changes at the Nickel site of the regulatory [NiFe] hydrogenase from *Ralstonia eutropha* detected by X-ray absorption spectroscopy. Biochemistry 42, 11004–11015.
[12] Winter, G., Buhrke, T., Lenz, O., Jones, A.K., Forgber, M. and Friedrich, B. (2005) A model system for [NiFe] hydrogenase maturation studies: Purification of an active site-containing hydrogenase large subunit without small subunit. FEBS Lett. 579, 4292–4296.

[13] Bradford, M.M. (1976) A rapid and sensitive method for the quantitation of microgram quantities of protein utilizing the principle of protein-dye binding. Anal. Biochem. 72, 248–254.
[14] Pettifer, R.F. and Hermes, C. (1985) Absolute energy calibration of X-ray radiation from synchrotron sources. J. Appl. Crystallogr. 18, 404–412.
[15] Dau, H., Liebisch, P. and Haumann, M. (2003) X-ray absorption spectroscopy to analyze nuclear geometry and electronic structure of biological metal centers – potential and questions examined with special focus on the tetra-nuclear manganese complex of oxygenic photosynthesis. Anal. Bioanal. Chem. 376, 562–583.
[16] Burgdorf, T., Löscher, S., Liebisch, P., van der Linden, E., Galander, M., Lendzian, F., Albracht, S.P., Meyer-Klaucke, W., Friedrich, B., Dau, H. and Haumann, M. (2005) Structural and oxidation state changes at its non-standard Ni–Fe site during activation of the NAD-reducing hydrogenase from *Ralstonia eutropha* detected by X-ray absorption, EPR, and FTIR spectroscopy. J. Am. Chem. Soc. 127, 576–592.
[17] Ankudinov, A.L., Ravel, B., Rehr, J.J. and Conradson, S.D. (1998) Real-space multiple-scattering calculation and interpretation of X-ray-absorption near-edge structure. Phys. Rev. B 58, 7565–7576.
[18] Yachandra, V.K. (1995) X-ray absorption spectroscopy and applications in structural biology in: Methods in Enzymologyy 246 – Biochemical Spectroscopy (Sauer, K., Ed.), pp. 638–678, Academic Press, New York.
[19] Gu, W., Jacquamet, L., Patil, D.S., Wang, H.X., Evans, D.J., Smith, M.C., Millar, M., Koch, S., Eichhorn, D.M., Latimer, M. and Cramer, S.P. (2003) Refinement of the nickel site structure in *Desulfovibrio gigas* hydrogenase using range-extended EXAFS spectroscopy. J. Inorg. Biochem. 93, 41–51.
[20] Colpas, G.J., Maroney, M.J., Bagyinka, C., Kumar, M., Willis, W.S., Suib, S.L., Mascharak, P.K. and Baidya, N. (1991) X-ray spectroscopic studies of nickel complexes, with application to the structure of nickel sites in hydrogenases. Inorg. Chem. 30, 920–928.
[21] Dau, H., Liebisch, P. and Haumann, M. (2005) The manganese complex of oxygenic photosynthesis: conversion of five-coordinated Mn(III) to six-coordinated Mn(IV) in the S_2–S_3 transition is implied by XANES simulations. Phys. Scr. T115, 844–846.
[22] Mijovilovich, A. and Meyer-Klaucke, W. (2003) Simulating the XANES of metalloenzymes – a case study. J. Synchrotr. Radiat. 10, 64–68.
[23] Jones, A.K., Lenz, O., Strack, A., Buhrke, T. and Friedrich, B. (2004) NiFe hydrogenase active site biosynthesis: identification of Hyp protein complexes in *Ralstonia eutropha*. Biochemistry 43, 13467–13477.
[24] Carepo, M., Tierney, D.L., Brondino, C.D., Yang, T.C., Pamplona, A., Telser, J., Moura, I., Moura, J.J. and Hoffman, B.M. (2002) 17O ENDOR detection of a solvent-derived Ni–(OH(x))–Fe bridge that is lost upon activation of the hydrogenase from *Desulfovibrio gigas*. J. Am. Chem. Soc. 16, 281–286.
[25] Meinke, C., Sole, V.A., Pospisil, P. and Dau, H. (2000) Does the structure of the water–oxidizing photosystem II–manganese complex at room temperature differ from its low-temperature structure? A comparative X-ray absorption study. Biochemistry 39, 7033–7040.